Sādhanā, Vol. 26, Parts 1 & 2, February–April 2001, pp. 5–24. © Printed in India

Segregation in cast products

A GHOSH

Department of Materials and Metallurgical Engineering, Indian Institute of Technology, Kanpur 208 016, India
e-mail: ahin@iitk.ac.in

Abstract. Microsegregation gets eliminated significantly if subsequent hot working and/or annealing are done on cast products. Macrosegregation however persists, causing problems in quality, and hence, has to be attended to. Microsegregation is a consequence of rejection of solutes by the solid into the interdendritic liquid. Scheil's equation is mostly employed. However, other equations have been proposed, which take into account diffusion in solid phase and/or incomplete mixing in liquid.

Macrosegregation results from movements of microsegregated regions over macroscopic distances due to motion of liquid and free crystals. Motion of impure interdendritic liquid causes regions of positive macrosegregation, whereas purer solid crystals yield negative macrosegregation. Flow of interdendritic liquid is primarily natural convection due to thermal and solutal buoyancy, and partly forced convection due to suction by shrinkage cavity formation etc.

The present paper briefly deals with fundamentals of the above and contains some recent studies as well. Experimental investigations in molten alloys do not allow visualization of the complex flow pattern as well as other phenomena, such as dendrite-tip detachment. Experiments with room temperature analogues, and mathematical modelling have supplemented these efforts. However, the complexity of the phenomena demands simplifying assumptions. The agreement with experimental data is mostly qualitative.

The paper also briefly discusses centreline macrosegregation during continuous casting of steel, methods to avoid it, and the, importance of early columnar-to-equiaxed transition (CET) as well as the fundamentals of CET.

Keywords. Macro- and microsegregation; cast products; continuous casting; columnar-to-equiaxed transition (CET).

1. Introduction

During solidification of liquid metals and alloys, crystals formation takes place. The resulting morphology has certain characteristics peculiar to cast structures. Morphology includes both *macrostructure* and *microstructure*.

Again, segregation of solutes also occurs upon freezing of alloys. Segregation refers to non-uniformity of chemical composition. The patterns of distribution of solutes in the resulting solid (i.e. segregation pattern) may really be considered as its 'chemical structure'. Development of morphology and segregation pattern are interlinked phenomena. Segregation also is subdivided into *macrosegregation* and *microsegregation*.

The topic has been reviewed in books dealing with solidification, and in this work some of them have been used extensively (Flemings 1974; Ghosh 1990). Some review papers are also available (Moore 1984; Ohnaka 1988; Flemings 1990; Roy *et al* 1992; Ghosh 1997). In addition, some recent research papers will also be referred to as required. Original references of earlier studies are omitted for the sake of brevity.

The basic principles of formation of microsegregation in castings and ingots were understood more than fifty years ago (see Flemings 1974). These were extended thirty years ago to include the quantitative description of diffusion in the solid during solidification. Later refinements have been made, including treatment of dendrite tip undercooling and extension of the treatment of microsegregation to complex, multicomponent alloys. Localised microsegregation causes macrosegregation as a result of physical movement of liquid and solid phases, most important being flow of interdendritic liquid.

Microsegregation results from freezing of solute-enriched liquid in the interdendritic spaces. But it does not constitute a major quality problem, since the effects of microsegregation can be removed during subsequent soaking and hot working. Macrosegregation, on the other hand, is non-uniformity of composition in the cast section on a larger scale. For example, a high degree of positive segregation in the central region of a continuously cast (CC) section is known as centreline segregation, and poses quality problems.

Figure 1 presents a typical carbon segregation pattern in a CC steel slab. The problem of centreline segregation has been found to be more serious in high carbon steels. This segregation of solute elements, expecially carbon, results in inconsistent transformation products (i.e. martensite, bainite) during subsequent hot working, and causes non-uniformity in mechanical properties of the finished product. Also, centreline segregation is known to be the prime source of subsurface cracks and porosity in CC products.

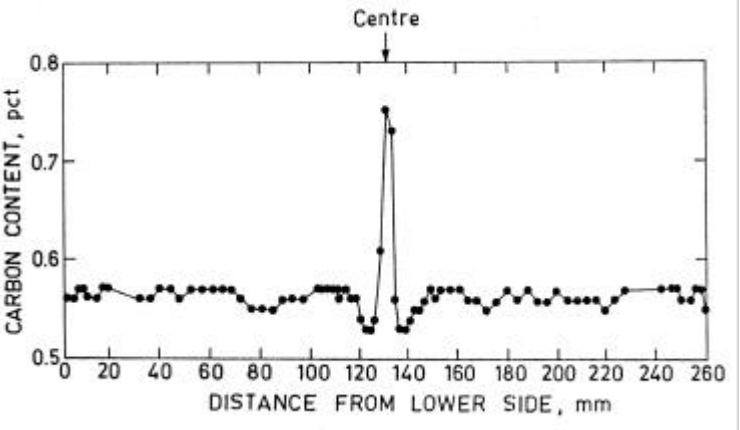

Figure 1. A typical concentration profile in an earlier continuous slab casting (Moore 1984).

It may be noted that in figure 1 the concentration profile is not smooth but is marked by random oscillations. These fluctuations occur on macro- and semi-macro scales. These are the consequence of the manner in which segregated spots get distributed. Such distribution is again closely linked with morphological features (i.e. grain structure) of the cast section. Technique of chemical analysis for segregation has a lot to do with the resulting profile. The traditional method has been drilling at selected spots and chemical analysis of the drillings. Large size thin sections give better mean values. More detailed concentration distribution can be obtained qualitatively by sulphur print, and quantitatively by etch print-cum-image analysis or by electron probe macroanalyser (EPMA).

2. Segregation fundamentals and their applications

2.1 *The fundamentals (Ghosh 1990)*

The basic cause of segregation is that the liquid rejects solutes during freezing because the solid has less solubility for them as compared to the liquid. If an impure liquid is kept in contact with its solid at the freezing temperature for an appreciable time, equilibrium partitioning of the solutes would be attained between the liquid and the solid. It may then be written that

$$C_S/C_L = K_e, \tag{1}$$

where C_S and C_L are concentrations of a specific solute (say i) in solid and liquid respectively, and K_e is known as *Equilibrium Partition Coefficient*. K_e is less than 1.

In diffusion and mass transfer, concentration of component $i(C_i)$ is per unit volume (say, g moles/cm^3 or g/cm^3). However, for solutes in dilute solutions, g/cm^3 would be proportional to weight percent of component $i(W_I)$. Hence, in the area of solidification, C_i mostly refers to W_i.

From a strict thermodynamic point of view,

$$K_e = a_s/a_L, \tag{2}$$

where a_s and a_L are activity of solute i, whose segregation is under consideration. Solutes in dilute binary solutions obey Henry's Law, where $a_S \propto C_5$, and $a_L \propto C_L$. On the basis of the same, (1) is justified. However, it has to be kept in mind that interactions with other solutes have be considered, and K_e, as defined by (1), should be modified.

Again, strictly speaking, K_e is a function of temperature, However, This can be ignored without much error for solutes at low concentrations. Table 1 presents some values of K_e for solidification of binary iron alloys into *d*-iron and *g*-iron. The lower the value of K_e, the more the tendency towards segregation. Hence, sulphur and oxygen are most segregating, while carbon and phosphorus also exhibit significant segregation.

For equilibrium (i.e. reversible) solidification,

$$C_S f_S + C_L f_L = C_O, \tag{3}$$

where f_S and f_L denote fraction of solid and liquid respectively and C_O is the total amount of a specific solute.

Equilibrium solidification assumes complete mixing in both liquid and solid at every stage of freezing. It also assumes equilibrium at the interface of solid and liquid. Since the interfacial process during solidification is very simple from an atomistic point of view,

Table 1. Values of K_e for solidification of binary iron alloys.

	K_e	
Element	*d*-Iron	*g*-Iron
Al	0·92	–
C	0·13	0·36
Cr	0·95	0·85
H	0·32	0·45
Mn	0·84	0·95
Mo	0·80	0·60
Ni	0·80	0·95
N	0·28	0·54
O	0·02	0·02
P	0·13	0·06
Si	0·66	0·5
S	0·02	0·02
Ti	0·14	0·07
V	0·90	–

assumption of interfacial equilibrium is justified. Mixing in liquid is primarily by convection and hence it may be quite fast. Therefore assumption of complete mixing in the liquid is often reasonable. Mixing in solids is by diffusion, which is a very slow process. Therefore assumption of complete mixing in solids is not a valid one except in some rare cases. Based on the above considerations, various combinations of assumptions have been made and several equations proposed.

With the assumption of complete mixing in the liquid phase and no diffusion in the solid, the following *solute redistribution equation* is obtained.

$$r = C_L/C_O = (1 - f_s)^{K_e - 1}. \tag{4}$$

This is known as Scheil's equation. r is a measure of solute segregation (i.e. enrichment) of the liquid with progressive solidification.

A more realistic assumption is incomplete mixing in liquids. Based on the material balance of solute across a thin strip of thickness dx parallel to a plane interface, it may be derived that

$$dC_L/dt = D(d^2C_L/d^2x') + R(dC_L/dx'), \tag{5}$$

where x' is distance from the solid/liquid interface, which itself is moving with time. R is the linear velocity with which the interface is moving (i.e. linear rate of solidification), and t is time from beginning of solidification.

R is a function of time. Hence the solution of (5) requires computer-aided numerical methods. However Burton and others (Ghosh 1990) analytically solved it by taking R as constant. Enrichment of liquid based on *Burton's equation* may be written as

$$C_L/C_O = (1 - f_S)^{k_{\text{eff}} - 1}, \tag{6}$$

where

$$K_{\text{eff}} \approx K_e/\{K_e + (1 - K_e)\exp(-R/k_m)\}, \tag{7}$$

and k_m is mass transfer coefficient. If $R/k_m \ll 1$, i.e. for slow solidification and/or vigorous stirring, $K_{\text{eff}} \approx K_e$ (Scheil's equation). If $R/k_m \gg 1$, $K_{\text{eff}} \approx 1$, i.e. $C_L \approx C_O$ and there is almost no segregation. This is the situation in rapid solidification.

2.2 *Application to microsegregation (Flemings 1974)*

During solidification, the entire mass consists of 3 regions, viz. solid, liquid and solid–liquid mixture. The last one is known as the *mushy zone* and consists of *dendrites* and *interdendritic liquid*. Positive microsegregation occurs in the interdendritic liquid due to solute rejection from solidifying dendrites.

It has been well-established for several decades that the composition of a solidified dendrite is not uniform. Traditionally, it is known as *coring*. The core is the purest since it is the first to solidify. Solidification leads to progressive enrichment of the interdendritic liquid with solutes. This results in progressive increase of solute concentration in the dendrite from the core to its periphery.

If the dendrites are small in size, then interdendritic liquid in the mushy zone may be assumed to be completely mixed. In such a situation, Scheil's equation has been employed as the basis of quantitative analysis. Brody and Flemings took into consideration diffusion in solid dendrites and modified Scheil's equation as follows (Flemings 1990).

$$C_S^* = K_e C_L = K_e C_O \{1 - f_S/(1 + aK_e)\}^{\frac{K-1}{e}}, \tag{8}$$

where

$$a = 4D_S t_f / d^2, \tag{9}$$

D_S is diffusivity of the solute in solid, t_f is solidification time and d is the dendrite arm spacing. The analysis is approximate and valid only for small values of a.

Figure 2 (Flemings 1974) shows calculated segregation of phosphorus in d-iron. The dotted line shows interface concentration and the solid line shows final composition. The difference represents extent of solid diffusion.

Segregation causes rejection of solutes by the solid with consequent enrichment of the remaining liquid. This often leads to secondary reactions, such as formation of oxides, sulphides, oxysulphides and nitrides during freezing. Such reactions can significantly alter microsegregation patterns (Ghosh 1990).

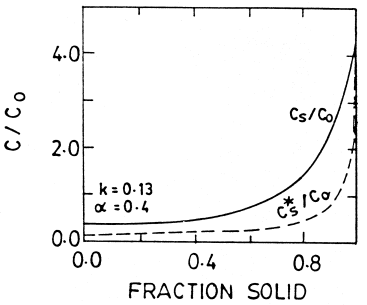

Figure 2. Calculated segregation of phosphorus in d-iron (Flemings 1990).

Lacaze & Lesoult (1999) have reported both experimental investigations as well as theoretical analysis of microsegregation during solidification of an Al–Cu–Mg–Si alloy. Alloys were directionally solidified from the bottom, and quenched after some time. Mg and Cu were analysed at various longitudinal and transverse locations with a microprobe analyser. In quenched samples, each horizontal section corresponded to a certain fractional solidification (f_s). Cumulative average Cu-concentration is plotted as a function of f_s in figure 3. Data were averaged as well as corrected for physical noise of X-ray emission. The calculated curve in figure 3 is according to the Gulliver–Scheil model, which takes into account solute diffusion both in solid and liquid.

2.3 *Application to macrosegregation*

Bulk motion of fluid is complex during solidification. Moreover, complete mixing in bulk liquid is not obtained. Hence, as such, the simple equations noted above are not normally applicable. However, they have been occasionally employed with reasonable predictions. Some examples are given below.

Freezing of a rimming steel ingot is characterized by vigorous stirring due to gas evolution. It is approximated by plane-front solidification. Nilles (Ghosh 1990) analysed sulphur segregation in such a situation, and found good correlation between theoretically calculated values of k_m, with those estimated from experimental data with the help of (6) and (7). Ohnaka (1988) suggested modifications to Scheil's equation to incorporate effect of bulk flow, and proposed the following,

$$r = C_L/C_O = (1 - f_S)_e^{(K-1)/x}, \tag{10}$$

where x is a factor to take account of influence of flow, which depends on this situation. Choudhary & Ghosh (1994) employed ratio of sulphur to carbon segregation indices to test these. Both Scheil's equations and (10) yield,

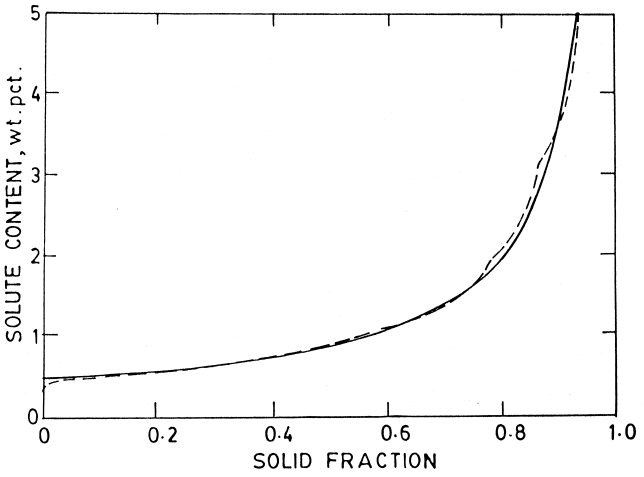

Figure 3. Distribution of solute as calculated with the Gulliver–Scheil model (full line) and cumulative distribution obtained from the experimental points (dashed line) (Lacaze & Lesoult 1999).

$$\ln r_S / \ln r_C = (K_e^S - 1)/(K_e^C - 1) = B = \text{a constant}, \tag{11}$$

where r_S and r_C are segregation indices of sulphur and carbon respectively in continuous casting of steel billets. Value of B is equal to 1·225 from table 1. Figure 4 shows comparison of (11) with experimental data. There is a lot of scatter, which is usual in these studies. In spite of that the average experimental value of $1n\, r_S/1n\, r_C$ matched closely with (11) at columnar-to-equiaxed transition (CET), but not for the centreline. The explanation is that, up to CET, columnar zone advances as a sort of plane front, but in central equiaxed zone it is not the case.

3. Fundamental studies on macrosegregation

3.1 *Introduction*

As already stated that localized microsegregation causes macrosegregation as a result of physical movement of liquid and solid phases, most important being flow of interdendritic liquid. It is a complex phenomenon. Many variables affect macroscopic distribution of a solute in a cast product, important ones being: size of casting, rate of solidification, mode of heat extraction, composition of the material, and superheat. For example, patterns would depend on whether it is sand casting, ingot casting in metallic mould or continuous casting. Hypoeutectic, eutectic and peritectic alloys, binary and multicomponent system would exhibit different patterns.

Distribution of macrosegregation in the cast product are measured by cutting sections of solidified product, and chemically analysing samples from different locations. However, flow of liquid in interdendritic space as well as in the bulk is difficult to visualize and quantitatively measure. Hence, experimental data on alloys are not adequate and satisfactory even now. In order to circumvent it, experiments have been carried out in transparent room temperature analogues. A well-studied system is the aqueous solution of NH_4Cl. A large volume of mathematical modelling work has also been reported, especially

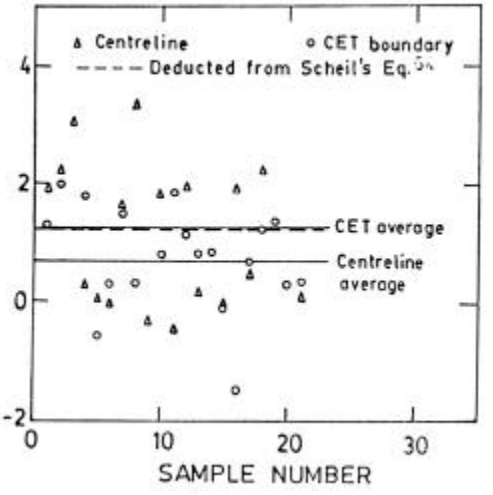

Figure 4. $\text{Ln}r_s/\text{ln}r_c$ values of billet samples for the centreline and CET boundary (Choudhary & Ghosh 1994).

in recent years. Besides ingot and continuous casting, several fundamental studies have been carried out with Pb–Sn alloys. This system offers advantages, such as low melting temperature, a simple and well-established phase diagram, and precise knowledge of properties.

Fluid flow during solidification is principally by natural convection caused by density gradient in the liquid. Such density gradient arises, first of all, from temperature gradient in the liquid, and leads to *thermal convection*. Due to rejection of solutes into the interdendritic liquid, concentration and consequent density gradients are set up in the liquid. This is known as solutal buoyancy, and the resulting convective flow as *solutal convection*. In most situations, both are significant, and the resulting convection has been termed *thermo-solutal* convection or *double diffusive* convection.

Forced convection arises typically from suction caused by solidification shrinkage. Electromagnetic forces or centrifugal acceleration are also occasionally imposed. Exudation of interdendritic liquid onto the surface has also been observed. It may also be influenced by solid movement, such as bulging and consequent development of voids along the centreline during continuous casting. Interdendritic liquid is impure. Hence, *positive macrosegregation* occurs, wherever it concentrates due to its motion. The solid in the mushy zone is primarily rigidly held with the rest of solidified mass. However, free crystals also form due to detachment from dendrite tips, as well as in the equiaxed zone. Wherever these concentrate, we have *negative macrosegregation*, since these are relatively pure.

The purpose of mathematical modelling is manifold, viz. prediction of microstructure, macrostructure, microsegregation, macrosegregation, temperature profile, rate of solidification etc. Application of basic segregation equations to microsegregation and macrosegregation has been illustrated in §2. When it comes to prediction of macrosegregation, mathematical modelling exercises have also to be concerned with heat flow and temperature profile, solid/liquid interface profile, as well as flow of liquid in the solidifying casting, besides segregation equations. The complexity of the situation demands simplifying assumptions. A separate discussion on this is beyond the scope of the present paper. Flow of interdendritic liquid also calls for physical description of the mush, adding to complexity and uncertainties in analysis.

Flemings and his coworkers (Flemings 1974) were the earliest to attempt a mathematical model of macrosegregation. Scheil's equation was employed for microsegregation. The flow of interdendritic liquid was expressed by Darcy's Law for flow through a porous medium. Recently Singh & Basu (2000) have briefly reviewed the modelling of convection in the mushy zone and its effect on macrosegregation. It can be treated as a porous medium where the solid is stationary, and is valid for the columnar zone.

Alternatively, the mush can be considered as a mixture of solid crystals and liquid. In this case the movement of both solid and liquid is permitted, and this representation is closer to the equiaxed mode of solidification. The moving solid and liquid mixture can be treated as a single phase with variable viscosity formulation in macroscopic flow calculations. Some recent formulations allow relative motion between these phases.

Solutal and thermal buoyancy forces may either augment or oppose one other, depending on the relative densities of the alloy constituents and the particular constituent with which the interdendritic liquid becomes enriched as solidification proceeds. For

example, in Al–4·5 wt% Cu alloy, the primary solid phase is aluminium-rich, whereas the interdendritic liquid becomes enriched in copper, the denser of the two constituents. Therefore, solutal and thermal buoyancy forces augment each other.

The relative strengths of solutal and thermal buoyancy forces in the mushy zone are represented by a buoyancy parameter N, given by

$$N = b_S \cdot \Delta C_L / b_T \cdot \Delta T = b_S / m b_T, \tag{12}$$

where b_S and b_T are respectively the solutal and thermal expansion coefficients of the fluid and m is the slope of the liquidus line on the equilibrium phase diagram ($m = \Delta T/\Delta C_L$). For $N > 0$, solutal buoyancy augments thermal buoyancy. Conversely, they oppose each other, if $N < 0$. For $-1 < N < 0$, solutal buoyancy partially offsets thermal buoyancy. If $N < -1$, solutal buoyancy opposes and totally dominates. These are shown schematically in figure 5 (Prescott & Incropera 1996).

N is also related to the ratio of *solutal Rayleigh number* (Ra_c) and *thermal Rayleigh number* (Ra_T), where

$$\mathrm{Ra}_C = g b_S G_C H^4 / D_C n, \tag{13}$$

$$\mathrm{Ra}_T = g b_T G_T H^4 / K_T n. \tag{14}$$

Hence

$$\mathrm{Ra}_C / \mathrm{Ra}_T = b_S / m b_T \cdot K_T / D_C = N \cdot K_T / D_C. \tag{15}$$

Here g is acceleration due to gravity, G_C and G_T are respectively solutal and thermal gradients, H is characteristic length, n kinematic viscosity, K_T thermal conductivity and D_C solute diffusivity in the liquid.

3.2 *Unidirectional solidification*

Unidirectional solidification is the simplest geometry. Several laboratory investigations have been conducted with static melts unidirectionally solidified by cooling from the

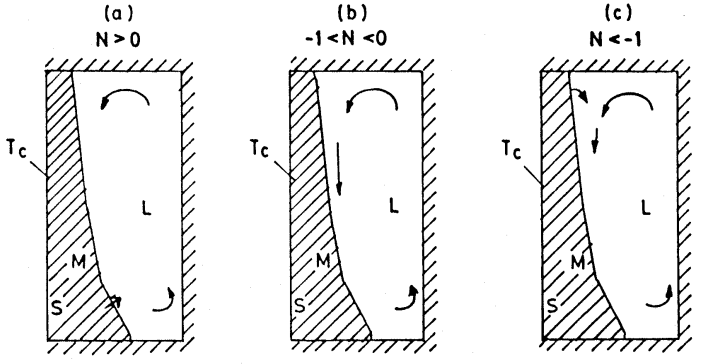

Figure 5. Thermosolutal convection pattern in the melt and mushy zone of a solidifying alloy: (**a**) solutal buoyancy forces augmenting thermal buoyancy force, (**b**) solutal buoyancy forces opposing thermal buoyancy forces, with thermal buoyancy dominating in the mushy zone, and (**c**) solutal buoyancy forces opposing and dominating thermal buoyancy forces in the mushy zone (Prescott & Incropera 1996).

bottom. Since temperature increases in the upward direction, liquid is denser towards the bottom. Hence thermal buoyancy opposes upward motion of the liquid.

As far as macrosegregation is concerned, Bergman *et al* (1997) studied Pb–Sn alloys, which were bottom cooled at various cooling rates (i.e. temperature gradients). Modified Rayleigh number (Ra_m) was employed as the ratio of the driving solutal buoyancy force to retarding Darcy frictional force. Increasing Ra_m was found to increase longitudinal segregation, decreased freckle trails and increased channel formation.

Li *et al* (1999) also studied Pb–Sn alloys, cooled from the bottom. In hypoeutectic Pb–15wt% Sn and Pb–36% of Sn, interdendritic liquid would be enriched in Sn, and hence lighter than bulk liquid, causing upward convection. The situation is the reverse in hypereutectic. Pb–85% Sn alloy. It was established that more the upward flow, more is macrosegregation (figure 6). In figure 6, C_O is nominal Sn concentration of alloys, $\overline{C}$ is persumably the average value of C at any horizontal section, f_S was taken as equal to L/L_O, where L_O is the length of ingot and L is vertical distance from the bottom. It was also found that the solutal gradient was by and large restricted to the interdendritic liquid. In the bulk melt above the mush, composition was almost uniform, but was enriched in Sn due to upward flow and mixing of interdendritic liquid.

Prescott & Incropera (1996) studied the freezing of Pb–19wt% Sn alloy in vertical cylindrical moulds. Cooling was horizontal and radial, which was unidimensional, but not unidirectional. Thermal and solutal buoyancy were opposing. Within the mushy zone, solutal buoyancy was calculated as to be 14 times larger than the thermal buoyancy force. Sn concentration was measured around the circumference in transverse section. As figure 7 shows, there was considerable variation of concentration along the circumference, demonstrating that macrosegregation was not axisymmetric. This was persumably due to flow asymmetry etc. Numerical simulation failed to predict this asymmetry.

Singh & Basu (1995) and Basu & Singh (1997) carried out numerical simulation of freezing of Fe–1% C alloy in a rectangular cavity. Heat flux was unidirectional and horizontal, normal to one opposing set of vertical walls. The other walls were to be assumed insulating and thermosolutal convection was assumed. It was a continuum formulation covering mushy zone and bulk liquid. Macrosegregation profiles for carbon at various stages of solidification exhibited formation of A-segregates etc. Apart from generating profiles; they have also reported the following segregation parameters.

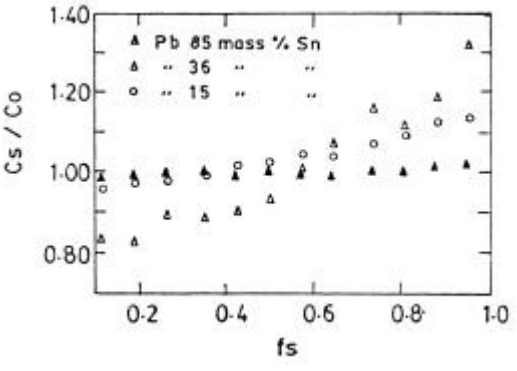

Figure 6. The longitudinal macrosegregation for Pb–Sn binary alloys upward directionally solidified under the conditions of R = 0·93 cm/h and G = 36·5 K/cm (Li *et al* 1999).

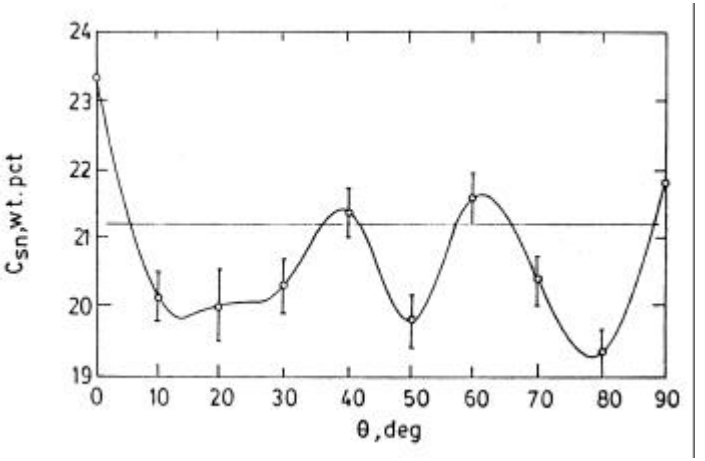

Figure 7. Circumferential variation of measured Sn concentration at $r^* = 0{\cdot}30$ and $z^* = 0{\cdot}83$ (Prescott & Incropera 1996).

(1) Severity of segregation, i.e. the difference between maximum and minimum nodal concentration ($C_{max} - C_{min}$) in the entire cavity.
(2) Area under segregation bands, 0·8–1·2% *C*, $C > 1{\cdot}2\%$, $C > 0{\cdot}8\%$.
(3) *Global extent of segregation (GES)*, which is defined as root mean square of deviation from nominal composition for all the nodal points, i.e.

$$\% \text{ GES} = 100/C_O[\Sigma\Sigma(\Delta C)^2 \mathrm{d}x\mathrm{d}y/\Sigma\Sigma \mathrm{d}x\mathrm{d}y]^{1/2}. \quad (16)$$

All these indices were found to decrease with increasing heat flux. This was attributed to decrease in mush length with increasing heat size. Schneider & Beckermann (1995) also carried out numerical simulation of melt solidification in similar rectangular cavities. However, they considered austenitic stainless steel containing 10 elements and involving a peritectic reaction. Macrosegregation profiles showed channel segregates etc. GES of an element was found to be linearly dependent on its partition coefficient, although such scaling was not possible locally.

3.3 *Ingot casting*

Macrosegregation patterns in common ingot casting are well-established. For the sake of brevity, the case of killed steel ingot will be very briefly presented. A killed steel ingot exhibits positive macrosegregation in the form of *V-segregates* and *A-segregates*. There is a bottom cone of negative segregation. It has been established that there is a strong thermal convection in the central pool of liquid. Positive segregations are due to flow through interdendritic channels and the negative segregation zone is caused by settling down of free, purer crystals (Ghosh 1990). When the flow is very strong, the positive macrosegregation zones form massive channels, known as *channel segregates*. Room temperature transparent models have demonstrated these flows and channel formations (Prescott & Incropera 1996). Numerical simulations based on these have predicted the A-segregates. However, the bottom negative segregation has not been predicted or observed in any simulation studies.

Recently, Yamada *et al* (1995) investigated solidification in 8-tonne sand mould ingots of high purity CrMoV steel grades. Experimental data were supplemented by theoretical analyses as well as laboratory experiments with small unidirectionally solidified melts. There was large macrosegregation of carbon, which depended on steel grade. Effective partition coefficients, as obtained from unidirectional solidification experiments, were found to be small, and were attributed to dominance of formation of *d*-Fe. Pseudo-binary phase diagrams were constructed for precise theoretical estimation of K_e for carbon. The results showed good match with those obtained from experiments. The velocity of the interdendritic liquid was also calculated.

Gu & Beckermann (1999) have reported experimental measurements of carbon and sulphur segregation along the vertical centreline of microalloyed medium carbon steel industrial ingots. Numerical simulation showed a qualitative match with positive segregation towards the top, but could not predict negative segregation at the bottom (figure 8).

Radovic *et al* (1999) made experimental measurements on 3-tonne high carbon, low alloy steels, and also carried out theoretical calculations. Relationships between chemical compositions of steel and liquid density changes were calculated. Influence of primary and secondary dendrite spacing on flow velocity *vis-à-vis* intensity of positive macrosegregation was examined. Global segregation index (GES) was found to vary linerly with interdendritic flow velocity for both C and S (figure 9).

4. Centreline segregation in continuous casting of steel

4.1 *Zone refining action*

Ghosh (1990, 1997) has reviewed this elsewhere in detail. As stated in §3 the Scheil equations, original and modified, as well as that of Burton have been occasionally

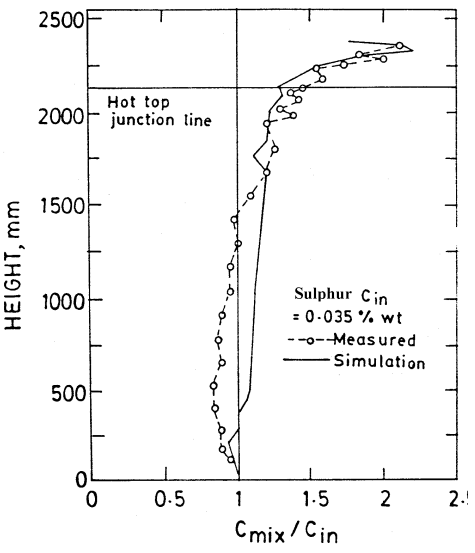

Figure 8. Comparison of measured and predicted macrosegregation variation of sulphur along the vertical centreline of the ingot (Gu & Beckermann 1999).

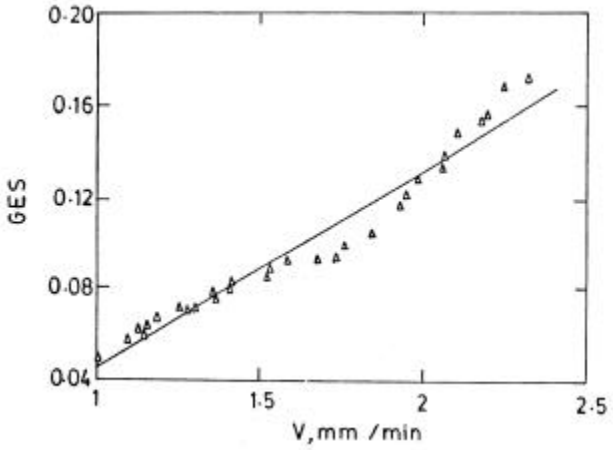

Figure 9. Global macrosegregation intensity of carbon as a function velocity of interdendritic liquid (Radovic *et al* 1999).

employed to predict macrosegregation in ingots and continuous casting with some success. If the solidification proceeds as columnar growth, the solidification front may be approximately treated as a plane front and (6) and (7) may be employed. Figure 10 shows the results of such calculation for carbon segregation with two assumed values of R/k_m. High positive centreline segregation is predicted. This is known as *'zone refining' action.* The only effective way to counter this is to promote formation of the equiaxed zone as early as possible during solidification. Formation of equiaxed crystals simultaneously over a region around the centreline stops further advance of the columnar zone, disperses the microsegrated spots throughout and prevents zone refining action.

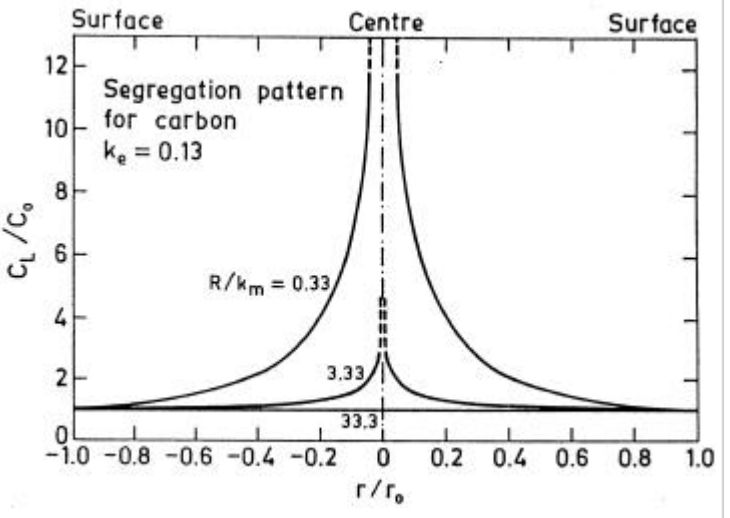

Figure 10. Transverse segregation profile for carbon in CC product calculated from Burton's equation (Ghosh 1990).

4.2 *Suction of interdendritic liquid*

Interdendritic liquid is impure. Hence its suction into the centreline region during solidification further aggravates the centreline segregation. The ideal pool profile during continuous casting is schematically shown in figure 11 (Ghosh 1990, 1997). This geometry allows feeding of cavities, due to shrinkage etc., by fresh liquid from the top, thus lowering build up of centreline segregation. However, generally this ideal situation is not achieved. An extreme case is what is known as *'Mini-ingot' formation*, and is shown schematically in figure 12.

As already stated, considerable fluctuations in composition occur in the longitudinal direction along the centreline. Mini-ingotism is a major contributor to this. The solidification front does not advance smoothly. Rather it proceeds by jerks or pulsations. Pulsations are caused by:

(a) Fluctuating nature of surface heat transfer coefficient and consequent fluctuations in heat flow;
(b) eddies and other flow instabilities;
(c) jerky withdrawals, mould oscillations etc.

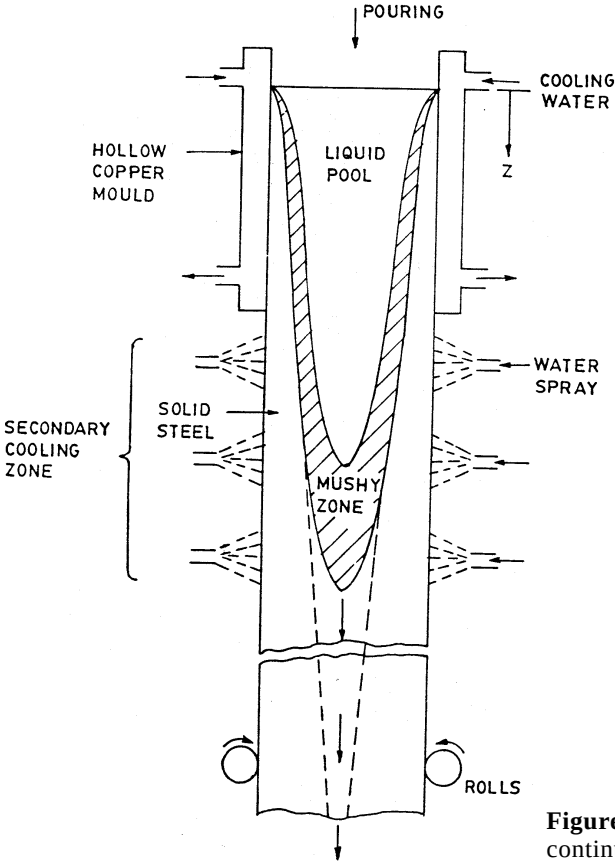

Figure 11. Ideal pool profile in continuous casting process (Ghosh 1990).

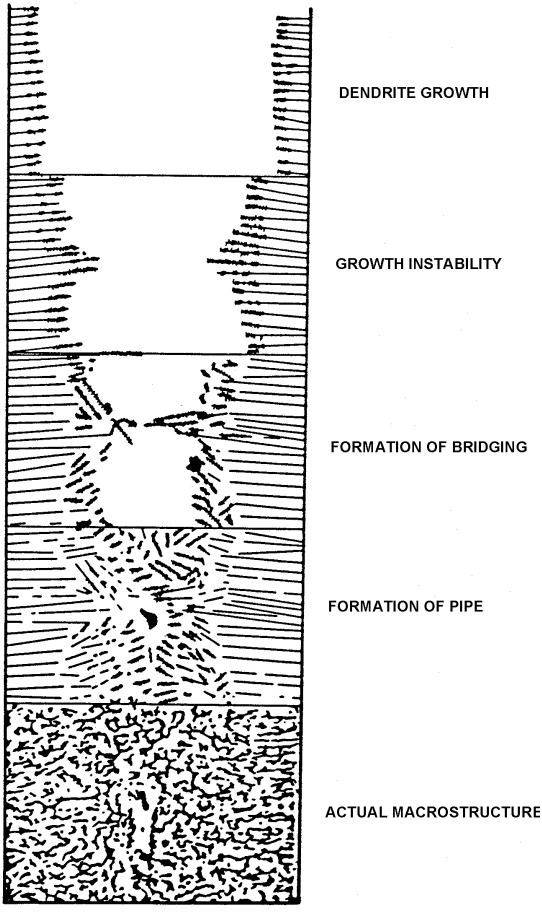

Figure 12. Formation of mini-ingot in continuous casting (Moore 1984).

As a consequence of this, columnar fronts often advance up to the centreline and form bridges, thus preventing feeding of shrinkage cavities below by fresh liquid. This causes suction of impure interdendritic liquid from the surrounding mushy zone into the central region thus increasing centreline segregation. Centreline porosity develops if feeding is not complete.

It has been established that bulging of the solid shell due to pressure at withdrawal rolls aggravates centreline segregation. If the shell bulges outwards, a cavity is created in the central liquid region thus enhancing suction. Heat transfer calculations have revealed that in the bottom part of the secondary cooling zone, centreline temperature decreases more rapidly than the surface temperature. This causes relatively more thermal contraction in the central region than at the surface, which in turn induces interdendritic liquid to flow towards the centreline, thus further aggravating suction.

4.3 *Equiaxed zone and its importance*

As already stated, the formation of equiaxed zones prevents refining action and thus helps to lower centreline segregation. As far as suction is concerned, again equiaxed zones are

beneficial since they do not allow bridge formation by columnar grains. However, large equiaxed dendrite crystals also tend to form partial bridges (Moore 1984). Therefore, equiaxed crystals should be small in size. The beneficial effect of equiaxed zones is well-established. Although there are several parameters governing centreline segregation, the relative values of segregation ratio (r) are determined primarily by K_e. Figure 13 demonstrates the same. K_e = 0·13, 0·02, 0·13 and 0·84 for C, S, P and Mn respectively (table 1). Hence, sulphur segregates the most and Mn the least.

4.4 *Control of centreline segregation*

Ghosh (1997) has reviewed this as well as other topics on continuous casting of steel in detail elsewhere, and hence only a brief mention of them will be made below.

The first feature of control of centreline segregation is to minimize the high positive segregation along the centreline. Promotion of formation of equiaxed zones as early as possible is a major step, and is facilitated by low superheat, medium carbon steel, electromagnetic stirring, and large section size. These tend to make the bulk temperature in the melt uniform during freezing, thus promoting formation of equiaxed grains.

Prevention of suction is achieved by one or more of the following:

(1) Low casting speed;
(2) adjustment of roll gap taper;
(3) soft reduction in cross-section of slab during the final stage of solidification;
(4) controlled plane reduction.

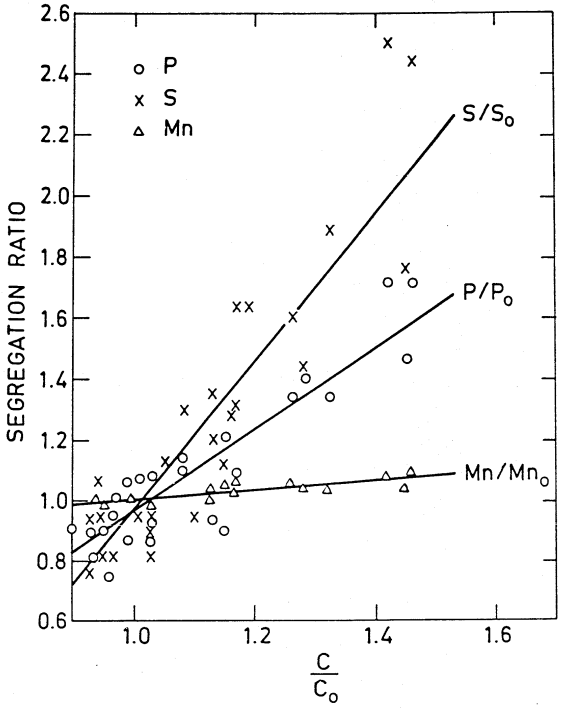

Figure 13. Relationship between segregation ratios of S, P and Mn with that of carbon in cast billets (Moore 1984).

A combination of the above strategies have almost eliminated centreline macrosegregation in continuous casting of steel in advanced plant practices. In recent years, therefore, more emphasis is being given on achieving desirable patterns in the segregated region. A principal breakthrough in quantitative evaluation of segregation distribution has come about with the development of electron probe *macroanalyser*. It is able to accommodate a large section (100 mm × 100 mm) for examination and can determine chemical composition of a spot ranging in size from 10 microns to 250 microns approximately from emitted X-rays (Tsuchida *et al* 1984).

The broad features of macrosegregation in longitudinal section of traditionally cast CC steel products are shown schematically in figure 14 (Goyal & Ghosh 1992). These are common features and get revealed even by ordinary sulphur prints. Dark regions have positive segregation of sulphur. U-segregation bands are associated with mini-ingot structure (i.e. severe centreline segregation), V-segregation bands occur at medium segregation levels, and V-lines at low positive segregation.

With modern practices, where centreline macrosegregation (on average) is very low or absent, the features shown in figure 14 have almost disappaeared. Instead, positively segregated masses tend to get dispersed over a large central zone as spots of small size. These are known as *semi-macro spot segregation*. For good properties, these spots should be less than 2 to 3 mm in diameter. Alternative structures are fine randomly placed V-lines (i.e. V-aggregates), which however are perhaps not as good as the former. Fine equiaxed dendrites are desirable, and can be achieved by addition of calcium and rare earths as grain refiners. Equiaxed dendrites are partly present as network and partly as free crystals. The latter are undesirable, since they tend to settle towards the bottom of the pool and give rise to undesirable *white bands*.

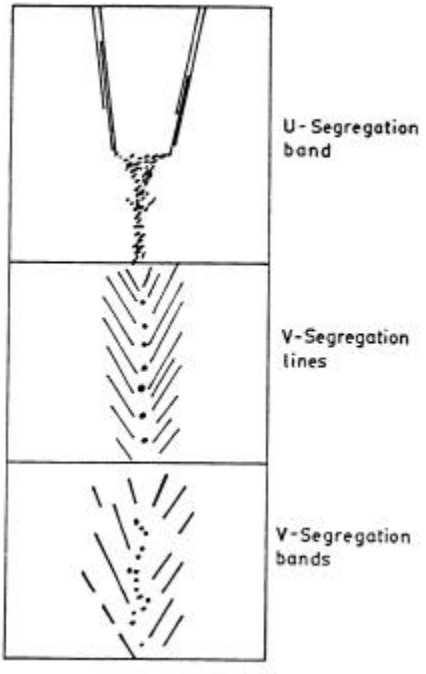

Figure 14. Some features of macrosegregation in longitudinal section of continuously cast billets (Goyal & Ghosh 1992).

Several mathematical models have been reported in literature on centreline segregation as well as on corrective practices. The earliest one is that by Miyazawa & Schwerdtfeger (1981) on bulging by pressure of withdrawal rolls and consequent enhancement of centreline segregation. However, this topic is omitted for concision.

5. Columnar-to-equiaxed transition (CET)

In view of the importance of the equiaxed zone, fundamentals of columnar-to-equiaxed transition will be briefly reviewed here. Flood & Hunt (1988) have reviewed the topic. Equiaxed grains grow ahead of columnar dendrites. They are also dendrites, but have no preferred orientation. Columnar-to-equiaxed transition (CET) occurs when the equiaxed grains are sufficiently large in size and number to impede the advance of the columnar front. The extent of the equiaxed zone is the result of competition between the relative growth rates of columnar and equiaxed grains. The formation of an equiaxed zone requires both the following:

(i) Presence of nuclei in bulk, and
(ii) conditions that promote their growth relative to columnar dendrites.

In the 1960s and 1970s, the tendency was to explain trends in CET only in terms of different mechanisms for the supply of equiaxed nuclei. However, recent papers have emphasized the growth aspects as well. Three mechanisms have been proposed for supply of nuclei for equiaxed growth:

- Constitutional supercooling (CS) driven heterogeneous nucleation;
- big bang mechanism;
- dendrite detachment mechanism.

It seems that none of these mechanisms can be ruled out and sometimes more than one is important.

In the big bang mechanism, crystals are supposed to break loose from the outer chill zone due to fluid motion and consequent impact. These free crystals act as substrates for equiaxed growth. Some experimental evidence for this is available. Ohno and his co-workers observed the appearance of neck-shaped crystals on the mould walls in some tin–bismuth alloys (Ghosh 1990). Through photographic studies they demonstrated that such neck-shaped crystals got detached under the action of convection. Occurrence of this behaviour was accompanied by formation of more equiaxed crystals.

Several experimetal studies have supported the dendrite detachment mechanism. Dendrite arms are supposed to break loose from the columnar zone due to partial melting caused by local fluctuations of temperature. Recalescence phenomena and turbulence also seem to be causing this phenomenon.

Several theoretical treatments are available in literature presenting analysis of growth processes. The important ones are those by Flood & Hunt (1988), Fredriksson & Olsson (1986), Lipton *et al* (1983). None of these have taken into consideration the important processes of sedimentation of grains and convective motion satisfactorily. Out of these, the model by Hunt and his co-workers (Flood & Hunt 1988) is the most popular one because

the analysis is simple and provides some quantitative criteria for CET. It assumes steady state growth and relates CET to columnar dendrite tip undercooling (ΔT_C).

It suggests that the structure will be fully columnar if

$$G_T > 0{\cdot}617(100N_O)^{1/3}[1 - (\Delta T_N/\Delta T_C)^3]{\cdot}\Delta T_C, \tag{17}$$

and fully equiaxed if

$$G_T < 0{\cdot}617(N_O)^{1/3}[1 - (\Delta T_N/\Delta T_C)^3]{\cdot}\Delta T_C, \tag{18}$$

where

$$\Delta T_C = [-8\Gamma m_L(1 - K_E)C_O{}^U/D]^{1/2}. \tag{19}$$

N_O = no. of nuclei per unit volume, ΔT_N is critical undercooling for nucleation on a substrate, and Γ is the Gibbs–Thompson coefficient. G_T is temperature gradient ahead of solidification front.

The undercooling required for CET has been found to be small. Therefore, roughly speaking, CET will occur as soon as the superheat is removed from a narrow layer ahead of the advancing columnar front. Choudhary & Ghosh (1994) collected continuously cast billet samples from Tata Steel, from which they cut sections, macroetched and measured locations of the CET. Samples of steel were also collected by drilling from the CET boundary. Carbon and sulphur were determined in a C–S determinator. This allowed calculation of liquid temperature (T_L) at the CET boundary.

Choudhary & Mazumdar (1995) developed a conjugate fluid flow-heat transfer model for the billet casting. This allowed computation of temperature field at any cross-section during solidification. The points which gave the same temperatures as T_L of CET boundaries were determined. Figure 15 presents the comparison of measured radial CET locations (d_y) with calculated ones (d_x), after superheat correction due to temperature loss between tundish and mould. The agreement was good.

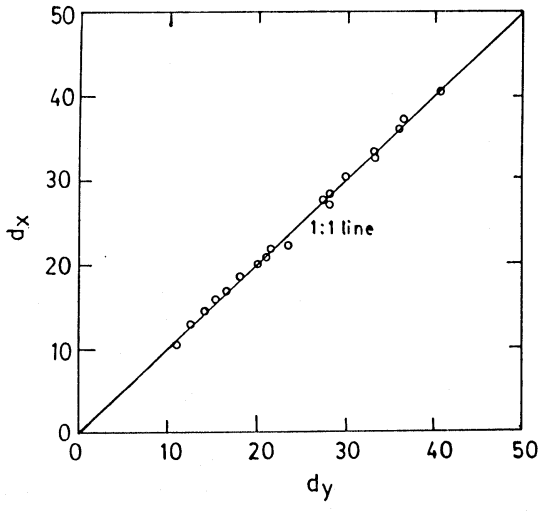

Figure 15. Comparison between measured and computed positions of CET boundary from the centre of billet samples with corrected pouring temperature (Choudhary & Ghosh 1994).

References

Basu B, Singh A K 1997 Role and characterization of double-diffusive convection during solidification of binary alloys. *Proc. 3rd ISHMT–ASME Heat & Mass Transfer Conf. and 14th Natl. Heat & Mass Conf.*, IIT, Kanpur, pp 129–141

Bergman M I, Fearn D R, Bloxham J, Shannon M C 1997 Convection and channel formation in solidifying Pb–Sn alloys. *Metall Mater. Trans.* A28: 859–866

Choudhary S K, Ghosh A 1994 A study of morphology and macrosegregation in continuously cast steel billets. *Iron Steel Inst. Jap. Int.* 34: 338–345

Choudhary S K, Mazumdar D 1995 Mathematical modelling of fluid flow, heat transfer and solidification phenomena in continuous casting of steel. *Steel Res.* 66: 199–205

Flemings M C 1974 *Solidification processing* (New York: McGraw Hill)

Flemings M C 1990 Segregation in castings and alloys. *Proc. Elliott Symp.* (Iron & Steel Soc) pp 216–235

Flood S C, Hunt J D 1988 Columnar to equiaxed transition. *Metals handbook* 9th edn (Am. Soc. Mater. Int.) vol. 15, pp 130–136

Fredriksson H, Olsson A 1986 Mechanism of transition from columnar to equiaxed zone in ingots. *Mater. Sci. Technol.* 2: 508–516

Ghosh A 1990 *Principles of secondary processing and casting of liquid steel* (New Delhi: Oxford & IBH) ch. 6,7 & 9

Ghosh A 1997 Fundamental aspects of segregation control in continuous casting of steel. *Proc. Int. Symp. on Quality Challenges in Continuous Casting* (Ranchi: Indian Inst. Metals), pp 203–218

Goyal R K, Ghosh A 1992 Centreline segregation in continuously cast steel billets. *Trans. Indian Inst. Metals* 45: 303–314

Gu J P, Beckermann C 1999 Simulation of convection and macrosegregation in a large steel ingot. *Metall. Mater. Trans.* A30: 1357–1367

Lacaze J, Lesoult G 1999 Modelling and development of microsegregation during solidification of an Al–Cu–Mg–Si alloy. *Iron Steel Inst. Jap. Int.* 39: 658–664

Li M, Mori T, Iwasaki H 1999 Effect of solute convection during macrosegregation in Pb–Sn binary alloys during upward directional solidification. *Iron Steel Inst. Jap. Int.* 39: 33–38

Lipton J, Kurtz W, Heinemann W 1983 *Concast Tech. News* 22: 4

Miyazawa K, Schwerdtfeger K 1981 Macrosegregation in continuously cast steel slabs – preliminary theoretical investigation on the effect of steady state bulging. *Arch. Eisenw.* 52: 415–422

Moore J J 1984 Review of axial segregation in continuously cast steel. *Continuous casting* (ed.) J J Moore (Iron & Steel Soc.) vol. 3, pp 11–20

Ohnaka I 1988 Microsegregation and macrosegregation. *Metals handbook* 9th edn (Am. Soc. Mater. Int.) vol. 15, pp 136–141

Prescott P J, Incropera F P 1996 Convection heat and mass transfer in alloy solidification. *Adv. Heat Transfer* 28: 231–328

Radovik Z, Lalovic M, Tripkovic M, Branislav J 1999 Forming of positive macrosegregation during steel ingot solidification. *Iron Steel Inst. Jap. Int.* 39: 329–334

Roy T K, Choudhary S K, Ghosh A 1992 *Tool and alloy steels* pp 365–372

Schneider M C, Beckermann C 1995 Simulation of micro-/microsegregation during solidification of a low-alloy steel. *Iron Steel Inst. Jap. Int.* 35: 665–672

Singh A K, Basu B 1995 Mathematical modelling of macrosegregation of iron carbon binary alloy: role of double diffusive convection. *Metall Mater. Trans.* B26: 1069–1081

Singh A K, Basu B 2000 On convection in mushy phase and its effect on macrosegregation. *Metall. Mater. Trans.* A31: 1687–1692

Tsuchida Y *et al* 1984 *Trans. Iron Steel Inst. Jap.* 24: 899

Yamada H, Takenouchi T, Takahashi T, Funazaki M, Iwadate T, Nakada S. 1995 Influence of alloying elements on the segregation of high purity CrMoV steel. *Iron Steel Inst. Jap. Int.* 35: 686–692